Studies of electron-molecule collisions: Applications to e-H_2O

Luiz M. Brescansin,[a] Marco A. P. Lima,[b] Thomas L. Gibson,[c] and Vincent McKoy
Arthur Amos Noyes Laboratory of Chemical Physics,[e] California Institute of Technology, Pasadena, California 91125

Winifred M. Huo[d]
Radiation Laboratory, University of Notre Dame, Notre Dame, Indiana 46556

(Received 18 March 1986; accepted 29 April 1986)

We report elastic differential and momentum transfer cross sections for the elastic scattering of electrons by H_2O for collision energies from 2 to 20 eV. These fixed-nuclei static-exchange cross sections were obtained using the Schwinger variational approach. In these studies the exchange potential is directly evaluated and not approximated by local models. The calculated differential cross sections, obtained with a basis set expansion of the scattering wave function, agree well with available experimental data at intermediate and larger angles. As used here, the results cannot adequately describe the divergent cross sections at small angles. An interesting feature of the calculated cross sections, particularly at 15 and 20 eV, is their significant backward peaking. This peaking occurs in the experimentally inaccessible region beyond a scattering angle of 120°. The implication of this feature for the determination of momentum transfer cross sections is described.

INTRODUCTION

Cross sections for the scattering of low-energy electrons by molecules play an important role in the modeling of gas lasers, planetary atmospheres, and swarm and plasma etching systems. In contrast to the related atomic problem, progress in both the experimental and theoretical studies of low-energy electron-molecule collisions has been limited.[1] On the theoretical side, this situation is primarily due to the additional complexities arising from the nonspherical potential fields of molecular targets. To date, most *ab initio* studies of electron-molecule collisions have hence concentrated on linear molecules where single-center expansion techniques are particularly well suited to exploit the cylindrical symmetry of such systems.[2–4] A multicenter method designed to be applicable to target molecules of arbitrary geometry would dramatically widen the range of problems amenable to theoretical study.

In this paper we present results of our studies of the cross sections for the elastic scattering of electrons by H_2O for incident energies from 2 to 20 eV. These cross sections were obtained in the fixed-nuclei and static-exchange approximations using a multichannel extension of the Schwinger variational principle which we have recently formulated.[1] A fixed-nuclei treatment of electron scattering by polar molecules is well known to lead to divergent cross sections due to the slow falloff of the T-matrix elements for large l.[5] This is an essential property of the dipole potential. This divergence can be removed only by introducing the nuclear motion through its rotational Hamiltonian. Although the high partial wave fixed-nuclei cross sections are divergent, the low partial wave fixed-nuclei results are directly useful since they can provide the differential cross sections at larger scattering angles. Furthermore, these fixed-nuclei cross sections for the low partial waves can then be appropriately augmented by laboratory-frame Born estimates for the higher partial wave contributions.[6,7] In contrast to these higher partial waves where the physics of the collision is essentially Born-like, the lower partial waves probe the short-range aspects of the potential field and are hence dynamically important. The static-exchange potential, which we use in these studies, can be expected to account well for these low partial wave collisions. We will, in fact, see that a comparison of our calculated cross sections with data over the experimentally accessible angular region, i.e., less than about 120°, bears this out particularly well. Furthermore, and more importantly, we will also see that our calculated differential cross sections rise significantly beyond 120° and are quite different from values which may be inferred from any extrapolation of the experimental data beyond 120°. Such differences in the differential cross sections can influence the derived values of momentum transfer cross sections.

An outline of the paper is as follows. In the next section we briefly discuss our Schwinger variational formulation of electron-molecule collisions. We then present several details of the applications of this theory to low-energy e-H_2O scattering and compare the resulting cross sections with available experimental data.

METHOD

Details of our Schwinger multichannel formulation of electron-molecule collisions have been discussed elsewhere[8,9] and only a brief outline will be given here. The Hamiltonian for the collision system can be written as

$$H = (H_N + T_{N+1}) + V = H_0 + V, \qquad (1)$$

where H_N is the target Hamiltonian, T_{N+1} is the kinetic energy operator of the incident electron, and V is the interac-

[a] Present address: Instituto de Física "Gleb Wataghin" Universidade Estadual de Campinas, 13100 Campinas, São Paulo, Brasil.
[b] Permanent address: Instituto de Estudos Avançados, Centro Técnico Aerospacial, 12200 São José dos Campos, São Paulo, Brasil.
[c] Present address: Department of Physics, Texas Tech University, Lubbock, Texas 79409.
[d] Mailing address: NASA–Ames Research Center, MS230-3, Moffett Field, CA 94035.
[e] Contribution No. 7381.

 0021-9606/86/161854-05$02.10

tion potential between the incident electron and the target, i.e.,

$$V=\sum_{i=1}^{N}\frac{1}{r_{i,N+1}}-\sum_{\alpha}\frac{Z_\alpha}{R_{\alpha,N+1}}. \tag{2}$$

In Eq. (2) the first and second terms are the electron repulsion and electron-nuclei attraction, respectively. The total scattering wave function satisfies the Schrödinger equation

$$(E-H)\Psi_{\mathbf{k}}=\hat{H}\Psi_{\mathbf{k}}=0. \tag{3}$$

To obtain a Schwinger variational principle for the multichannel scattering matrix associated with Eq. (3), we begin by introducing a projection operator P which defines the open-channel space in terms of the eigenfunctions of the target Hamiltonian H_N, i.e.,

$$P=\sum_{m=1}^{\text{open}}|\Phi_m(1,2,...,N)\rangle\langle\Phi_m(1,2,...,N)| \tag{4}$$

and

$$H_N\Phi_m=E_m\Phi_m,\quad E-E_m>0. \tag{5}$$

Note that the projector of Eq. (4) is different from the P operator of Feshbach formalism.[10] With this operator we obtain a projected Lippmann–Schwinger equation:

$$P\Psi_{\mathbf{k}}^{(+)}=PS_{\mathbf{k}}+PG_0^{(+)}V\Psi_{\mathbf{k}}^{(+)} \tag{6}$$

from

$$\Psi_{\mathbf{k}}^{(+)}=S_{\mathbf{k}}+G_0^{(+)}V\Psi_{\mathbf{k}}^{(+)}, \tag{7}$$

where $S_{\mathbf{k}}$ is the solution of the unperturbed Hamiltonian H_0, i.e., $\Phi_m(1...N)e^{i\mathbf{k}\cdot\mathbf{r}_{N+1}}$, and $G_0^{(+)}$ is the Green's function associated with E-H_0. Note that the continuum states of the target molecule must be included in $G_0^{(+)}$ in order to make the wave function $\Psi_{\mathbf{k}}^{(+)}$ on the left-hand side of Eq. (7) antisymmetric.[11]

We proceed by writing the Schrödinger equation in the form[9]

$$H\left[aP\Psi_{\mathbf{k}}^{(+)}+(1-aP)\Psi_{\mathbf{k}}^{(+)}\right]=0, \tag{8}$$

where a will be chosen to be $N+1$.[8,9] Insertion of Eq. (6) for $P\Psi_{\mathbf{k}}^{(+)}$ into Eq. (8), followed by rearrangement of the resulting expression, gives the multichannel equation $\Psi_{\mathbf{k}}^{(+)}$:

$$A^{(+)}\Psi_{\mathbf{k}}^{(+)}=VS_{\mathbf{k}}, \tag{9}$$

where

$$A^{(+)}=\frac{\hat{H}}{(N+1)}-\frac{P\hat{H}+\hat{H}P}{2}+\frac{PV+VP}{2}-VG_P^{(+)}V \tag{10}$$

and

$$G_P^{(+)}=\sum_{m=1}^{\text{open}}|\Phi_m\rangle g_m^{(+)}(\mathbf{r}_{N+1},\mathbf{r}'_{N+1})\langle\Phi_m| \tag{11}$$

with

$$g_m^{(+)}(\mathbf{r},\mathbf{r}')=-\frac{1}{2\pi}\frac{e^{ik_m|\mathbf{r}-\mathbf{r}'|}}{|\mathbf{r}-\mathbf{r}'|}. \tag{12}$$

Based on Eq. (9) we can write a multichannel variational functional for the scattering amplitude.

$$[f_{mn}]=-\frac{1}{2\pi}\frac{\langle\Psi_m^{(-)}|V|S_n\rangle\langle S_m|V|\Psi_n^{(+)}\rangle}{\langle\Psi_m^{(-)}|A^{(+)}|\Psi_n^{(+)}\rangle}. \tag{13}$$

Equation (13) is a multichannel extension of the usual Schwinger variational principle. Note that Eqs. (9) and (13) incorporate closed-channel effects without requiring the closed-channel Green's function which, in turn would have to include target continuum states. Expanding the variational scattering wave function in Eq. (13) in a basis of $(N+1)$-electron Slater determinants, this variational expression can be written as

$$f_{mn}=-\frac{1}{2\pi}\sum_{ij}\langle S_m|V|\Psi_i\rangle A_{ij}^{-1}\langle\Psi_j|V|S_n\rangle. \tag{14}$$

In this formulation all configurations representing both open and closed channels are treated equivalently. This variational formulation is obviously based on the variation of the total wave function rather than that of a specific scattering orbital. Finally, if we include only the Hartree–Fock wave function for the target state in expansion of P in Eq. (4), Eq. (13) reduces to the usual Schwinger variational expression for elastic scattering by a static-exchange potential.

Some important features of the variational principle in Eq. (14) are as follows. As in the original Schwinger principle,[12] an L^2 expansion of the trial wave function is possible and is assumed. Furthermore, if the orbitals appearing in the $(N+1)$-electron Slater determinants in the expansion of the scattering wave function are chosen to be Cartesian–Gaussian functions, all the matrix elements arising in Eq. (14), except those of $VG_P^{(+)}V$, can be evaluated analytically for a general molecular target. The matrix elements associated with the $VG_P^{(+)}V$ term can also be obtained analytically with an insertion-like quadrature around $G_P^{(+)}$, again using Cartesian–Gaussian functions. The "residue" contribution to these matrix elements of $VG_P^{(+)}V$ can be obtained essentially exactly via insertion of a complete set of plane waves around $G_P^{(+)}$. This procedure results in an S matrix that is very nearly unitary without resorting to large Cartesian–Gaussian insertion basis sets. Details of this plane wave insertion technique will be discussed elsewhere.[13]

Finally, we note that Eq. (13) provides an analytical approximation to the full-scattering amplitude in the body frame. To obtain the physical cross section one needs the laboratory-frame scattering amplitude. The partial wave decompositions arising in this frame transformation are carried out via a Gauss–Legendre quadrature.[14] This simply requires that the body-frame amplitudes be determined with the incoming and outgoing plane waves at an appropriate set of angles.

APPLICATIONS

In this section we discuss the results of our studies of the elastic-static exchange of e-H_2O scattering cross sections obtained using the Schwinger formulation outlined above. We will present elastic differential and momentum transfer cross sections for impact energies from 2 to 20 eV. These cross sections are obtained in the fixed-nuclei approximation.

It is convenient to construct the ground state SCF wave function using a large uncontracted (15s10p3d) Cartesian–Gaussian basis on the oxygen nucleus and a (6s1p) basis on the hydrogen nuclei. The exponents of these basis functions are shown in Table I. At the experimental equilibrium geom-

TABLE I. Cartesian Gaussian basis.[a,b]

Atom and type	Exponent
O(15s)	7816.54, 1175.82, 273.88, 81.1696, 27.1836, 9.5322, 3.4136, 0.9398, 0.2846, 0.0712, 0.0178, 0.004 45 0.0012, 0.0003, 0.0001
O(10p)	35.1832, 7.904, 2.3051, 0.7171, 0.2137, 0.054, 0.0135, 0.003 38, 0.000 84, 0.000 21
O(3d)	1.2188, 0.3610, 0.09
H(6s)	13.3615, 2.0133, 0.4538, 0.123, 0.02, 0.002
H(1p)	0.8371

[a] Cartesian Gaussian functions defined by $\chi^{(\alpha)}_{lmn} = N_{lmn}(x-A_x)^l(y-A_y)^m(z-A_z)^n e^{-\alpha|r-A|^2}$ where A locates the origin and N_{lmn} is a normalization constant.

[b] Basis set used for SCF wave function, expansion of the scattering functions, and for quadrature insertion in $VG_P^{(+)}V$ (see the text).

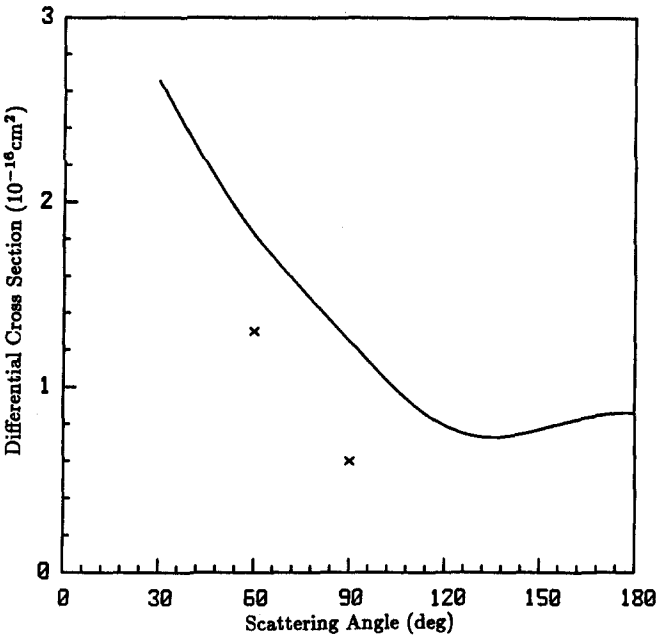

FIG. 1. Differential cross sections (DCS) for e-H_2O scattering at 2 eV: present static-plus-exchange (SE) results (solid line), static-model-exchange polarization (SMEP) results of Ref. 17 (×).

etry of R(O-H) = 1.81a_0 and θ(H-O-H) = 104.5°,[15] this basis gives an SCF energy of − 76.0545 a.u. With this basis set and molecular geometry, our calculated dipole moment is 0.784 a.u. compared with the experimental value of 0.724.[16] This basis provides a large number of virtual orbitals ($39a_1$, $4a_2$, $13b_1$, $20b_2$) which are used to expand the trial scattering wave function and to satisfy the closure relation assumed in the quadrature insertion technique for evaluating matrix elements of $VG_P^{(+)}V$. In the body frame all calculated amplitudes include contributions from $(N+1)$-electron Slater determinants of $^2A_1$, $^2A_2$, $^2B_1$, and $^2B_2$ symmetries. In the partial wave decomposition of the scattering amplitude we included terms with $l \leq 5$. To assess the possible sensitivity of these differential cross sections to the size of the basis, we also carried out calculations using smaller basis sets. These results suggest that the differential cross sections, which we will discuss below and which were obtained with 81 basis functions, are reasonably converged. For example, calculations with 73 basis functions led to changes of about 5% to 10% in these cross sections.

In Figs. 1–5 we show our calculated fixed-nuclei elastic differential cross sections for collision energies of 2, 6, 10, 15, and 20 eV along with the theoretical results of Jain and Thompson[17] and the experimental data of Danjo and Nishimura[18] and of Jung *et al.*,[19] where available. We report differential cross sections for angles beyond about 30° because, as discussed earlier, the scattering solutions are obtained with a large discrete basis which, although containing some very diffuse functions, cannot describe the higher partial waves which lead to the divergence in this region.

Although there is no experimental data at 2 eV with which to compare, our differential cross sections at this energy do show a shallow minimum around 130° with a slight increase at higher angles. This behavior is quite similar to what is seen in related studies of e-LiF by Norcross and Collins.[5] A comparison with the calculated results of Jain and Thompson,[17] using a static-model-exchange polarization potential, is not very meaningful since their cross sections are available at only two angles. At 6 eV our differential cross sections between 30° and about 80° differ considerably from the data of Danjo and Nishimura[18] which, in turn, are very different from the experimental values of Jung *et al.*[19] Reasons for either of these disagreements are not apparent at present. Our calculated cross sections between 80° and 120° agree well in both shape and magnitude with the measurements of Danjo *et al.*[18] The results of Jain and Thompson[17] at 60° and 90° are in good agreement with the data of Danjo and Nishimura.[18]

The calculated differential cross sections at 10, 15, and 20 eV, shown in Figs. 3–5, agree well with the experimental

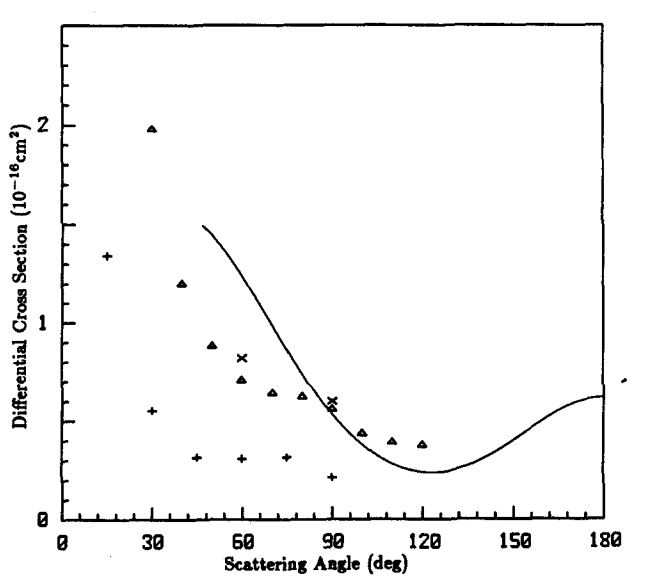

FIG. 2. DCS for e-H_2O scattering at 6 eV *f*: present SE results (solid line), SMEP results of Ref. 17 (×), measured values of Ref. 18 (Δ), measured values of Ref. 19 (+).

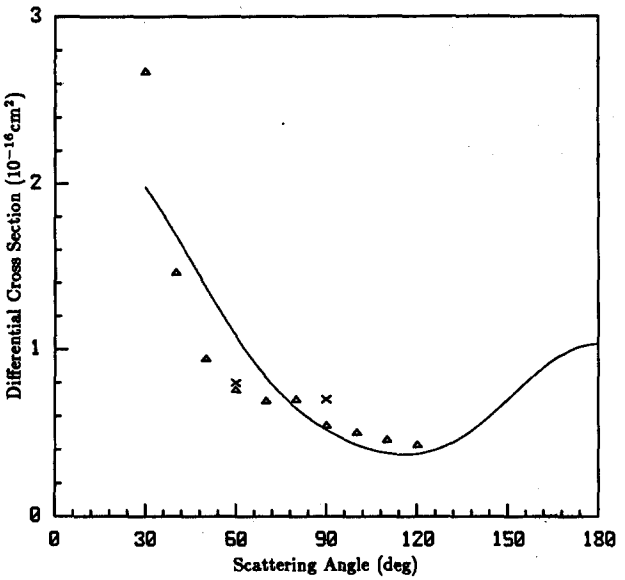

FIG. 3. DCS for e-H_2O scattering at 10 eV: present SE results (solid line), SMEP results of Ref. 17 (×), measured values of Ref. 18 (Δ).

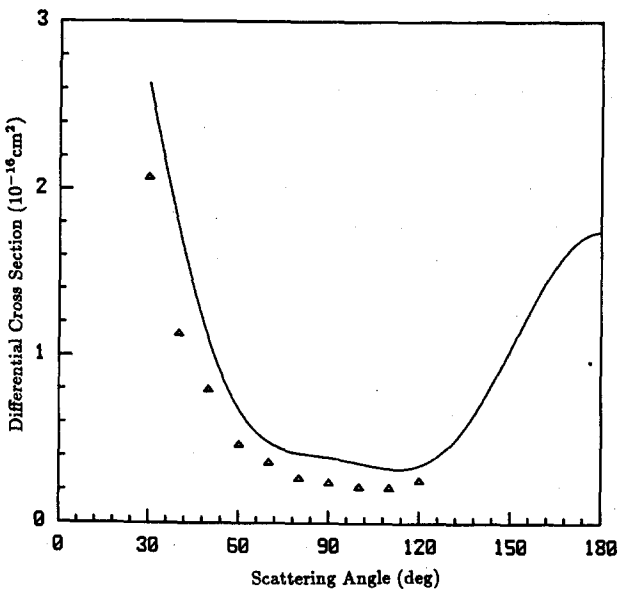

FIG. 5. DCS for e-H_2O scattering at 20 eV: present SE results (solid line), measured values of Ref. 18 (Δ).

data of Danjo and Nishimura.[18] The agreement between these calculated static-exchange and measured differential cross sections suggest that, at these energies and angular ranges, polarization effects are not important for this polar target. The experimental data again extends out only to 120°. Beyond 120° our cross sections show a significant backward peak which becomes more pronounced as the energy increases. This is probably the most important feature in these results. This backward peaking will obviously contribute significantly to the momentum transfer cross sections via the usual relationship, i.e.,

$$\sigma^M = 2\pi \int_0^\pi \frac{d\sigma}{d\theta}(1 - \cos\theta)\sin\theta\, d\theta. \tag{15}$$

Furthermore, a smooth extrapolation of the measured data beyond 120° would very likely seriously underestimate the total cross sections. Momentum transfer cross sections derived from the measured cross sections of Danjo and Nishimura,[18] assuming a smooth extrapolation of the data beyond 120° are shown in Fig. 6. The larger discrepancies between the calculated and "measured" momentum transfer cross sections seen at the higher energies in Fig. 6 are due to deficiencies in the extrapolated differential cross sections at larger angles. In fact, contributions from these angles dominate the momentum transfer cross sections. We expect that calculated differential elastic cross sections will generally prove very useful in the extrapolation of measured data to high, and experimentally inaccessible, angular regions.[20]

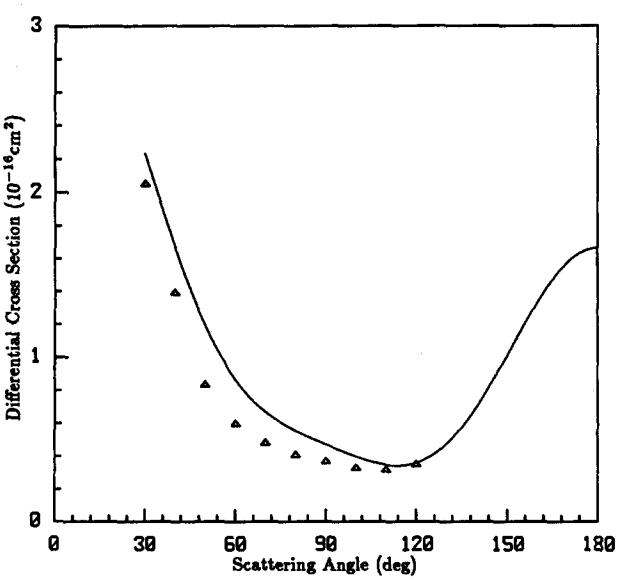

FIG. 4. DCS for e-H_2O scattering at 15 eV: present SE results (solid line), measured values of Ref. 18 (Δ).

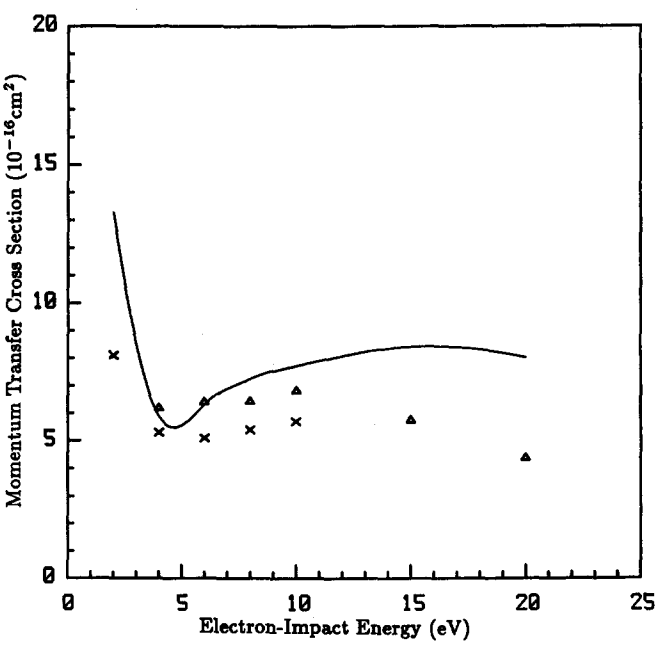

FIG. 6. Elastic momentum transfer cross section for e-H_2O scattering: present SE results (solid line), present SMEP results of Ref. 17 (×), measured values of Ref. 18 (Δ).

CONCLUSIONS

In this paper we have discussed the results of applications of the Schwinger variational method to the elastic scattering of low-energy electrons by H_2O. We have studied the differential and momentum transfer cross sections at the static-exchange level and for collision energies from 2 to 20 eV. Although these results were obtained using an expansion of the scattering wave function in a large discrete basis and hence cannot describe small angle scattering adequately, the calculated cross sections agree quite well with available experimental data. Furthermore, our differential cross sections show significant backward peaking, particularly at 15 and 20 eV. This behavior lies in the experimentally inaccessible region beyond 120° where any usual extrapolation of the experimental data below 120° would lead to estimates of the cross sections very different from the calculated results. Furthermore, the differential cross section at these high angles is strongly influenced by the short-range components of the scattering potential such as the exchange potential. For this reason, the present results obtained with the proper treatment of exchange can be useful in assessing model-exchange potentials. Finally, calculated differential cross sections at high angles will be particularly important in extracting momentum transfer cross sections from beam measurements.

ACKNOWLEDGMENTS

This material is based upon research supported by the National Science Foundation under Grant No. PHY-8212992 and by the NASA–Ames Cooperative Agreement No. NCC2-319. One of us (M. A. P. L.) acknowledges financial support from the Comissão Nacional de Energia Nuclear (CNEN), Rio de Janeiro, Brasil. L. M. B. acknowledges a fellowship from Conselho Nacional de Desenvolvimento Cientifico e Technológico (CNPq), Brasil. Two of us (M. A. P. L. and L. M. B.) acknowledge financial support from the Fundação de Amparo à Pesquisa do Estado de São Paulo (FAPESP), Brasil. The research of W. M. H. is supported by the National Aeronautics and Space Administration NASA–Ames Cooperative Agreement No. NCC2-147.

[1]See, for example, S. Trajmar, D. F. Register, and A. Chutjian, Phys. Rep. **97**, 219 (1983).
[2]N. F. Lane, Rev. Mod. Phys. **52**, 29 (1980).
[3]See, for example, B. I. Schneider and L. A. Collins, Phys. Rev. A **27**, 2847 (1983); J. Phys. B **18**, L857 (1985).
[4]R. R. Lucchese, K. Takatsuka, and V. McKoy, Phys. Rep. **131**, 147 (1986).
[5]See, for example, D. W. Norcross and L. A. Collins, *Advances in Atomic and Molecular Physics* (Academic, New York, 1982), Vol. 18, p. 341.
[6]N. T. Padial and D. W. Norcross, Phys. Rev. A **27**, 141 (1983).
[7]T. N. Rescigno, A. E. Orel, A. U. Hazi, and B. V. McKoy, Phys. Rev. A **26**, 690 (1982).
[8]K. Takatsuka and V. McKoy, Phys. Rev. A **24**, 2473 (1981); **30**, 1734 (1984).
[9]See, also, M. A. P. Lima and V. McKoy (unpublished results).
[10]H. Feshbach, Ann. Phys. (N. Y.) **19**, 287 (1962).
[11]S. Geltman, *Topics in Atomic Collision Theory* (Academic, New York, 1969), p. 99.
[12]B. A. Lippmann and J. Schwinger, Phys. Rev. **79**, 469 (1950).
[13]T. L. Gibson, M. A. P. Lima, W. M. Huo, and V. McKoy, Phys. Rev. A (to be published).
[14]M. A. P. Lima, T. L. Gibson, K. Takatsuka, and V. McKoy, Phys. Rev. A **30**, 1741 (1984).
[15]See, for example, L. C. Synder and H. Basch, *Molecular Wave Functions and Properties* (Wiley, New York, 1972).
[16]See, for example, W. Meyer, in *Modern Theoretical Chemistry*, edited by H. F. Schaefer III (Plenum, New York, 1977), Vol. 3, p. 442.
[17]A. Jain and D. G. Thompson, J. Phys. B **15**, L631 (1982).
[18]A. Danjo and H. Nishimura, J. Phys. Soc. Jpn. **54**, 1224 (1985).
[19]K. Jung, Th. Antoni, R. Müller, K. H. Kochem, and H. Ehrhardt, J. Phys. B **15**, 3535 (1982).
[20]See, for example, M. A. P. Lima, T. L. Gibson, W. M. Huo, and V. McKoy, Phys. Rev. A **32**, 2696 (1985).